Inorganica Chimica Acta, 188 (1991) 139–144

Ligand substitution pathways in carbonyl complexes of $Fe(dmgBF_2)_2$ with *trans* weak donor, sterically hindered and anionic ligands

Dennis V. Stynes*, D. G. A. Harshani de Silva and David W. Thompson
Department of Chemistry, York University, North York, Ont., M3J1P3 (Canada)

(Received May 14, 1991)

Abstract

The effects of weak donor ligands CH_3CN, dmso, dmf, thf, the sterically hindered ligand 2-methylimidazole (2-MeIm) and anionic ligands CN^-, Cl^-, Br^-, on the axial ligation reactions of *trans*-$FeN_4L(CO)$ complexes are described (N_4 = the tetradentate macrocyclic ligand bis-difluoro(dimethylglyoximato)-borate). In reactions with 1-methylimidazole (MeIm) in dichloromethane solution two dissociative paths (CO and L loss) contribute for the weak donors but only the CO loss path is important for the anionic or sterically hindered ligands studied. The relative binding constants of L to $FeN_4(CH_3CN)_2$ in CH_3CN or CH_2Cl_2 solution are $CN^- > MeIm > py > 2\text{-}MeIm \gg Cl^- > Br^- > CH_3CN$ and relative rates of CO dissociation *trans* to L are CN^-, $MeIm < py < CH_3CN$, $2\text{-}MeIm < Cl^-$, Br^-.

Introduction

The axial ligation reactions of FeN_4 systems have been extensively studied for a wide variety of macrocylic ligands N_4 and neutral axial ligands, CO, py, MeIm, RNC, PR_3, etc. and the delabilizing effects of π acceptor ligands well established [1–4]. Because of the strong Fe–CO bond and large *trans* delabilizing effect of CO in bis-dimethylglyoximato complexes of Fe(II), direct dissociation of L *trans* to CO has never been observed although it occurs as the exclusive path in ruthenium porphyrins [5] and phthalocyanines [6] and has occasionally been found in hemes [7] and other iron macrocycles [8] whose Fe–CO bonds are substantially weaker. In seeking examples of this 'base off' path within the dimethylglyoximate iron(II) system we have examined carbonyl complexes, $FeN_4L(CO)$, in which L is a very weak ligand or a sterically hindered ligand and N_4 is the bis-difluoro(dimethylglyoximato)borate ligand which provides facile entry into weak ligand complexes FeN_4L_2 [3]. The ability to probe two dissociative paths within a given complex is rare and provides a sensitive measure of the mutual bonding effects of ligands.

The sterically hindered 2-MeIm ligand has been used to confer a pentacoordinate high spin structure in hemes [9] and as a model for the strain proposed in the T-state of hemoglobin [7]. Unlike hemes, in the FeN_4 system a low spin $FeN_4(2\text{-}MeIm)_2$ complex is obtained.

Experimental

Materials

The complexes $FeN_4(CH_3CN)_2$, $FeN_4L(CO)$ (L = thf, dmf, dmso) and $FeN_4X(CO)^-$ (X = CN^-, Cl^-, Br^-) were prepared as described previously [3]. The chemicals $[(C_2H_5)_4N]Cl$, $[(C_2H_5)_4N]CN$, $[((CH_3(CH_2)_3)_4N]Br$, 1-methylimidazole and 2-methylimidazole (Aldrich) were used as received. CH_2Cl_2 was distilled from P_2O_5 and toluene from $LiAlH_4$. CH_3CN was reagent grade or better.

Physical measurements

Visible spectra were recorded using an Aminco DW-2a UV–Vis spectrophotometer. Extended photolyses were carried out using an 200 W quartz-halogen lamp at room temperature.

Kinetics

Slow reactions were carried out and analyzed as described previously [2a]. For biphasic reactions, the absorbance at 535 nm corresponding to the fast phase was obtained from A_∞ derived from a least-squares fit of absorbance data to first order kinetics. The fast reactions were studied and analyzed using an Applied Photophysics flash photolysis system [3] with photolysis of CO saturated solution of

---

*Author to whom correspondence should be addressed.

0020-1693/91/$3.50

$FeN_4L(CO)$ (L = py and 2-MeIm) in CH_2Cl_2 and in toluene, for 2-MeIm and py complexes, respectively, at 25 °C. The pentacoordinate FeN_4L is trapped efficiently as the FeN_4L_2 complex, and its fate was followed with time ($\lambda = 540$ nm for 2-MeIm and $\lambda = 520$ nm for py). Analysis of the increase in absorbance at $\lambda = 408$ nm for the formation of $FeN_4$2-MeIm(CO) and at $\lambda = 403$ nm for the formation of $FeN_4py(CO)$ are in agreement with that for the disappearance of FeN_4L_2.

Spectrophotometric titrations

Equilibrium constants were determined from spectrophotometric data in CH_2Cl_2 solution ([Fe] = 10^{-4} M) typically containing fixed [CH_3CN] (1.0 and 0.1 M) and varying concentrations of ligand L or where more convenient as for K_2 for 2-MeIm binding at fixed [2-MeIm] (0.003 and 0.01 M) and varying [CH_3CN]. Successive binding constants K_1 and K_2 were treated independently (since $K_1 \gg K_2$) and analysed by the Hill equation using a linear least-squares fit as described previously [2b].

Species were routinely identified based on characteristic MLCT bands in the visible spectra with λ_{max} (nm) as follows in CH_2Cl_2: $FeN_4(CH_3CN)$MeIm (488), FeN_4(2-MeIm)$_2$ (540), $FeN_4(CH_3CN)$(2-MeIm) (492), FeN_4py_2 (524), $FeN_4(CH_3CN)py$ (488), $FeN_4(CH_3CN)CN^-$ (490), $FeN_4(CH_3CN)Cl^-$ (392–448; broad band), $FeN_4(CH_3CN)Br^-$ (390–468; broad band), and $FeN_4L(CO)$ [3b] and $FeN_4X(CO)^-$ ($X = CN^-$, Cl^-, Br^-) as reported previously [3c].

Results and discussion

We have previously described a variety of weak donor complexes of FeN_4 and studies of their dissociative axial ligand substitution reactions in the neat donor solvents W = CH_3CN, dmso, dmf and thf [3b]. Reactions of the $FeN_4W(CO)$ complexes with MeIm in neat solvent W proceeds according to eqn. (1) via a rate determining step involving CO dissociation.

$$FeN_4(W)(CO) + 2MeIm \longrightarrow FeN_4(MeIm)_2 + W + CO \quad (1)$$

When W is also the solvent, the alternative path involving rate determining loss of W, will be suppressed. Therefore reaction (1) was investigated in CH_2Cl_2 solution to probe this alternative pathway.

Two-path reactivity of Fe(dmgBF$_2$)$_2$W(CO)

The two dissociative paths for reaction of $FeN_4W(CO)$ with excess MeIm are illustrated in Scheme 1. Loss of CO produces the transient pentacoordinate FeN_4W species, which in CH_2Cl_2 can be efficiently trapped by excess MeIm giving FeN_4(MeIm)W which reacts rapidly to give $FeN_4(MeIm)_2$. Dissociation of W however leads to an $FeN_4(CO)$ intermediate which would be trapped as the very inert FeN_4(MeIm)(CO) complex. Prolonged thermal reaction or photolysis will cleanly convert the FeN_4(MeIm)(CO) product to the $FeN_4(MeIm)_2$ species. The generation of the pink $FeN_4(MeIm)_2$ product via these two paths is easily distinguished based on the large difference in the rates of these two reactions.

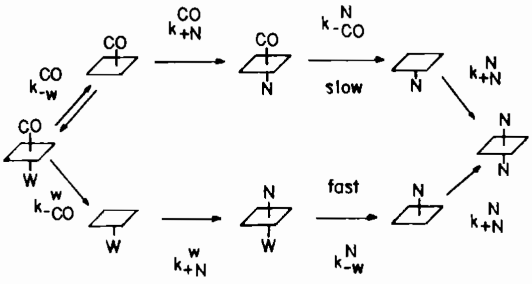

Scheme 1.

Under conditions of 100% efficient trapping of intermediates by MeIm the rate constants for the fast and slow phases are given by

$$k_{fast} = k_{-CO}{}^{W} + k_{-W}{}^{CO} \quad (2)$$

$$k_{slow} = k_{-CO}{}^{N} \quad (3)$$

The increased absorbance at 535 nm due to the bis(MeIm) product occurring during the fast and slow phases is related to the ratio of the dissociative rate constants for $FeN_4W(CO)$ since the two initial products FeN_4(MeIm)(CO) and $FeN_4(MeIm)_2$ are formed in the ratio of these rate constants.

$$\Delta A_{fast}/\Delta A_{slow} = k_{-CO}{}^{W}/k_{-W}{}^{CO} \quad (4)$$

Typical spectrophotometric data for the case W = CH_3CN are shown in Fig. 1(a) in which the intermediate FeN_4(MeIm)(CO) is clearly evident absorbing at 404 nm. In Fig. 1(b) the effect of added CH_3CN on the reaction is shown. In both cases the observation of isosbestic points is fully consistent with the formation of two products in a constant ratio with time. The reaction path involving loss of W will be suppressed in the presence of excess W based on the competition of W and MeIm for the $FeN_4(CO)$ intermediate but the path involving loss of CO is unaffected by excess W since both FeN_4W_2 and FeN_4(MeIm)W react rapidly with MeIm under the conditions of the experiment. The result is that both the rate in the fast phase and the relative product yields depend on the ratio [W]/[MeIm]. The appropriate equations simply require that the value

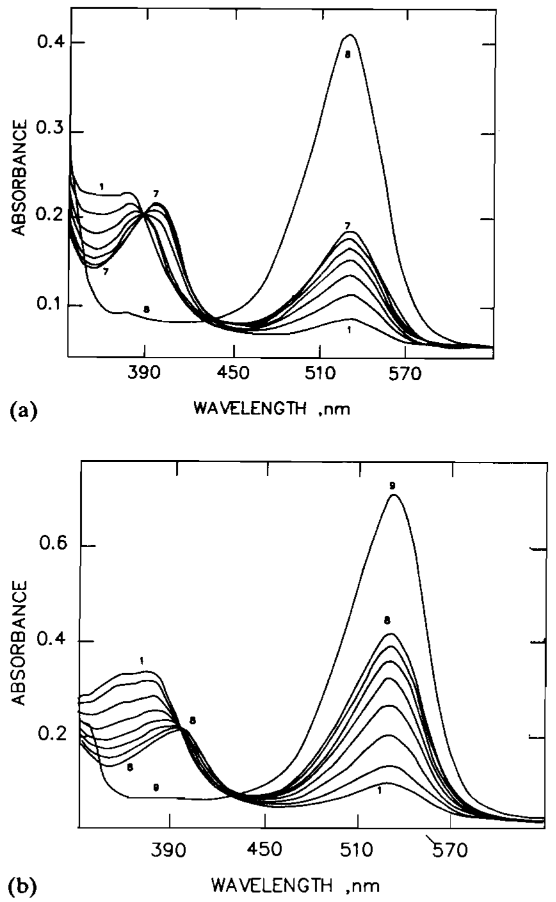

Fig. 1. (a) Spectral changes with time for the reaction of $FeN_4(CH_3CN)(CO)$ + MeIm ([MeIm] = 0.41 M) in CH_2Cl_2 containing 0.07 M CH_3CN. For increasing absorbances at 533 nm, times are 0, 300, 600, 990, 1530, 2370, 3750 s. The final spectrum was obtained after photolysis of the sample. (b) Spectral changes with time for the reaction of $FeN_4CH_3CN(CO)$ with MeIm ([MeIm] = 0.41 M) in CH_2Cl_2 containing 0.6 M CH_3CN at 25 °C. For increasing absorbances at 533 nm, times are 0, 210, 600, 1140, 1740, 2340, 3120, 4140 s. The final spectrum 9 was obtained from photolysis of the sample.

of k_{-W}^{CO} in eqns. (2) and (4) be multiplied by the fraction of the $FeN_4(CO)$ intermediate trapped by MeIm which we designate α.

$$\alpha = k_{+N}[\text{MeIm}]/(k_{+N}[\text{MeIm}] + k_{+W}[\text{W}]) \qquad (5)$$

Data for the thf, dmf, dmso and CH_3CN systems are collected in Table 1. In the CH_3CN case the values of k_{fast} are quite sensitive to [MeIm]/[W]. The appropriate plot of $1/(k_{fast}-k_{-CO}^{W})$ versus $[CH_3CN]/[MeIm]$ gives a straight line affording $k_{-A}^{CO} = 0.0017$ s^{-1} and $k_{+A}/k_{+N} = 0.4$. Analysis of the absorbance data according to eqn. (6) gives results in good agreement with the rate analysis. For the thf case the values of k_{fast} show a smaller variations with [W]/[MeIm] and the absorbance changes for the fast and slow phases afford a more accurate measure of the parameters. For dmso and dmf, the reaction involving CO loss makes up >75% of the unsuppressed case so no accurate measure of k_{+N}/k_{+dmso} was obtained. Data for the four systems are collected in Table 2.

$$\Delta A_{fast}/\Delta A_{slow} =$$
$$(k_{-CO}/k_{-W})(k_{+W}/k_{+N})[\text{W}]/[\text{N}] + (k_{-CO}/k_{-W}) \qquad (6)$$

TABLE 1. Kinetic dependence of k_{fast} on [W] for the reaction of $FeN_4(W)CO$ + MeIm in CH_2Cl_2 at 25 °C

[W]/[MeIm]	$k_{fast} \times 10^3$ (s^{-1})	A^{fast}/A^{slow}	$k_{-CO}^{W}/\alpha k_{-W}^{CO}$
W = CH_3CN[a]			
0	1.5 (0.05)	0.3 (0.04)	0.25 (0.05)
0.15	1.35 (0.06)	0.3 (0.05)	0.29 (0.07)
0.78	0.92 (0.02)	0.6 (0.05)	0.5 (0.1)
2.3	0.58 (0.02)	1.0 (0.15)	1.0 (0.2)
4.6	0.43 (0.02)	1.6 (0.34)	2.0 (0.44)
30.4	0.031		
W = thf[b]			
0	54 (4)	0.66 (0.11)	
1.5	46 (2)	0.91 (0.25)	
7.8	40 (5)	1.4 (0.3)	
19.3	32 (3)	3.0 (0.3)	
W = dmso			
0	34 (2)	8.1 (2)	
W = dmf			
0.1	1.3 (0.1)	2.8	
11.4	1.0 (0.1)	>15	

[a] [MeIm] = 0.4 M. [b] [thf] = 0.7 M.

As a test of the presumed dissociative scheme shown above, acetonitrile was used as a trapping ligand for the thf and dmso complexes. In a CO saturated solution at $[CH_3CN] = 0.1$ M one observes a clean single step reaction which goes completely to $FeN_4(CH_3CN)(CO)$ at a rate of 4×10^{-4} s^{-1}. This is considered to be in reasonable agreement with the sum of the two paths in Table 1 based on MeIm trapping. In the case of CH_3CN trapping, both paths give the final product in a single fast phase because the rate of reaction of $FeN_4(CH_3CN)_2$ with CO is fast. In the absence of excess CO an increase in absorbance at 440 nm is observed assigned to the $FeN_4(CH_3CN)_2$ complex (CO loss path) which subsequently reacts with the CO liberated in the initial reaction to give finally an equilibrium mixture of $FeN_4(CH_3CN)_2$ and $FeN_4(CH_3CN)(CO)$. This more complex kinetic behaviour was not subjected to detailed analysis. The corresponding reaction for the thf complex gave similar results in good agreement with expectations based on the dissociative scheme above.

The values of k_{-CO} in CH_2Cl_2 solutions are similar to those reported previously for reactions in neat

TABLE 2. Summary of kinetic data for the two-path mechanism in CH_2Cl_2 at 25 °C

W	k_{-W}^{CO} (s^{-1})	k_{-CO}^{W} (s^{-1})	k_{+N}^{W}/k_{+W}^{N}	k_{-W}^{CO}/k_{-CO}^{W}
CH_3CN	1.7×10^{-3}	0.3×10^{-3}	2.5 (0.6	5
dmso	0.4×10^{-3}	3.0×10^{-3}		0.1
dmf	0.3×10^{-3}	1.0×10^{-3}		0.3
thf	0.033	0.02	6 (1)	1.5

solvent W [3b]. Values of k_{-W}^{CO} for the three ligands indicate some differences in *trans* effects operate here since dmso is the most inert of the three *trans* to CO. It seems likely that a weak π donor character for dmso versus a weak π acceptor character for CH_3CN is responsible for these differences in lability *trans* to CO. It is noteworthy that all ligands investigated show dramatically reduced lability when *trans* to CO such that even the thf ligand would be classified as inert.

Steric effects

Imidazole* ligands with substituents in the 2 position suffer steric effects which are manifested in increased rates of ligand dissociation [7, 8], reduced equilibrium constants [10], and structural distortions [11] relative to unhindered cases. Stepwise ligation of 2-MeIm to $FeN_4(CH_3CN)_2$ (eqns. (7) and (8)) in dichloromethane may be observed by spectrophotometric titration affording equilibrium constants

$$FeN_4(CH_3CN)_2 + L \rightleftharpoons FeN_4L(CH_3CN) + CH_3CN \qquad K_1 \qquad (7)$$

$$FeN_4(CH_3CN)L + L \rightleftharpoons FeN_4L_2 + CH_3CN \qquad K_2 \qquad (8)$$

given in Table 3 (Fig. 2). Both constants are significantly reduced relative to an unhindered 1-MeIm ligand as seen in Table 3.

The steric effect resulting from mutually *trans* 2-MeIm ligands is also found in kinetic data for reaction of FeN_4L_2 with CO given in Fig. 3. Analysis of the data in terms of eqn. (9) for a classic D mechanism

$$1/k_{obs} = k_{+L}[L]/k_{-L}k_{+CO}[CO] + 1/k_{-L} \qquad (9)$$

gives $k_{-L} = 160 \pm 20$ s^{-1} and $k_{+L}/k_{+CO} = 22 \pm 5$. The 2-MeIm lability is approx. five orders of magnitude greater than for the unhindered 1-MeIm but the relative rates of addition to the pentacoordinate FeN_4(2-MeIm) complex are not especially unusual. This shows that the steric effect of the Me group is predominantly an Fe–2-MeIm bond weakening arising from its inability to be accommodated at closer distances because of non-bonded interaction of the 2-Me group with atoms in the N_4 ligand. The effects are comparable to those reported for an Fe(phthalocyanine) system [7] shown in Table 4.

TABLE 3. Equilibrium data for the binding of L to $FeN_4(CH_3CN)_2$ in CH_2Cl_2

L	K_1	K_2
py[a]	$1.85(0.1)\times10^4$	250(50)
MeIm	$>10^5$	$1(0.2)\times10^4$
2-MeIm	1600(100)	10(2)
CH_3CN	1	1
CN^-	$>10^5$[b]	
Cl^-	164(10)[b]	
Br^-	2.1(0.04)[b]	

[a] Reported values in toluene for K_1 and K_2 are 2.6×10^4 and 120 [3a]. [b] Reported values of K_1 in CH_3CN are $>10^5$, 10 and 0.1 M^{-1} for L = CN^-, Cl^- and Br^-, respectively [3c].

Reactions of FeN_4(2-MeIm)(CO) with MeIm (Fig. 4) and tosylmethylisocyanide (TMIC) were studied in CH_2Cl_2 to elucidate whether the 'base-off' pathway is important for sterically hindered ligands. The reactions proceed cleanly according to eqns. (10) and (11)

$$FeN_4(2\text{-MeIm})(CO) + 1\text{-MeIm} \longrightarrow FeN_4(1\text{-MeIm})(2\text{-MeIm}) \xrightarrow{\text{fast}} FeN_4(1\text{-MeIm})_2 \qquad (10)$$

$$FeN_4(2\text{-MeIm})(CO) + TMIC \longrightarrow FeN_4(2\text{-MeIm})(TMIC) + CO \qquad (11)$$

The base-off pathway is ruled out in eqn. (10) since the required product FeN_4(1-MeIm)(CO) reacts 100 times more slowly than the net rate of reaction (10). Reaction of the FeN_4(2-MeIm)(CO) with TMIC according to eqn. (12) verifies the predominance of the CO loss path since in this case FeN_4(2-MeIm)(TMIC) ($\lambda_{max} = 453$ nm) is inert.

---

*The hindered pyridine ligands 2-methylpyridine and collidine (2,4,6-trimethylpyridine) show effects when added to 10^{-4} M FeN_4A_2 solutions only at concentrations above 0.1 M and these effects were found to be fully consistent with and likely due to the binding of trace unhindered pyridine impurities (at about 1 ppt or less). The 2-cyanopyridine ligand was found previously to bind only via the nitrile group [3b].

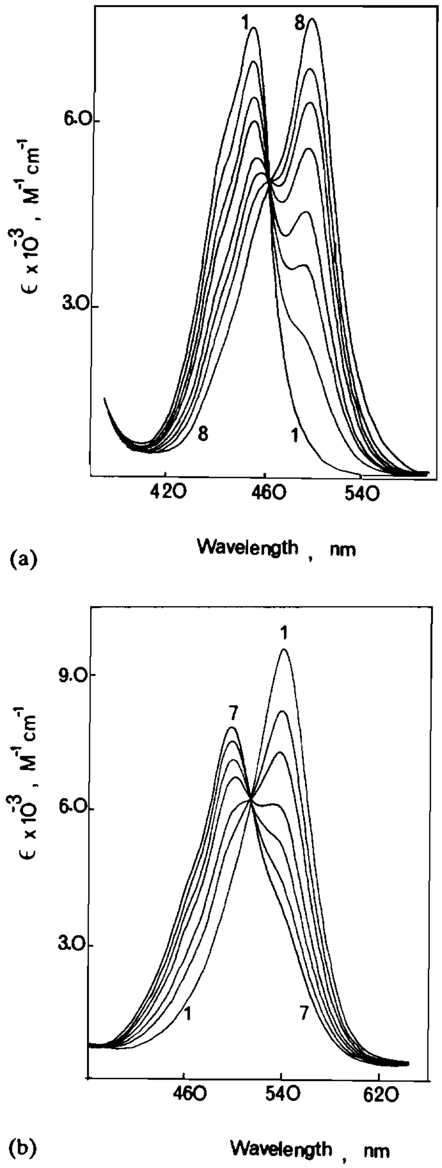

Fig. 2. (a) Spectroscopic data for the titration of $FeN_4(CH_3CN)_2$ (1.2×10^{-4} M) with 2-MeIm in CH_2Cl_2 solution containing 1.0 M CH_3CN at 25 °C. Spectra 1–8 are for [2-MeIm] = 0, 0.16, 0.313, 0.47, 0.79, 1.11, 1.56 and 3.2 mM, respectively. (b) Spectroscopic data for the titration of a solution of CH_2Cl_2 containing $FeN_4(CH_3CN)_2$ (9.5×10^{-5} M) and 0.01 M 2-MeIm, with CH_3CN solution at 25 °C. Spectra 1–7 are for [CH_3CN] = 0, 0.032, 0.064, 0.13, 0.19, 0.315, 0.47 M, respectively.

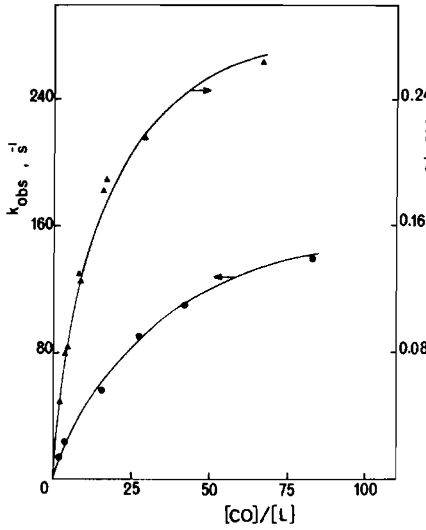

Fig. 3. Dependence of k_{obs} on the [CO]/[L] ratio for the reaction $FeN_4L_2 + CO \rightarrow FeN_4L(CO) + L$ in CH_2Cl_2 for L = 2-MeIm (●) (in toluene for L = py (▲)) at 25 °C.

While 2-MeIm experiences a significant steric effect in the FeN_4 system when bound *trans* to a itself, it remains the more tightly bound ligand when bound *trans* to CO or CH_3CN. It is also clear from data for a deuterohemedimethylester system studied by Traylor and co-workers [7] that the steric effect of 2-MeIm does not alter the favored path which is L loss in this case. ($k_{-CO}{}^{L}$ versus $k_{-L}{}^{CO}$ are 0.45 versus 150 s^{-1} for L = 2-MeIm and 0.028 versus 2.6 s^{-1} for L = Im). The numbers for the heme system nicely illustrate how the steric effect of 2-MeIm is almost equally distributed between the two *trans* ligands. The explanation for these effects is contained in the synergistic nature of the CO and imidazole bonding [2b] as well as the tendency for structural distortions of the tetradentate ligand which relieve strain on one side to introduce it on the opposite side.

Anionic ligands

The binding of the anions CN^-, Br^- and Cl^- to $FeN_4(CH_3CN)_2$ in CH_3CN solution and their effects on CO bonding have been described elsewhere [3c]. Reactions of these anionic carbonyl complexes $FeN_4X(CO)^-$ ($X = Cl^-$ and Br^-) with 1-MeIm are found to proceed exclusively via the CO loss path as evidenced by a single rate process ($k = 2.8\times10^{-3}$ s^{-1} and 2.1×10^{-3} s^{-1}, respectively) identified with reaction according to eqn. (12). Photochemical reaction of the cyano complex goes exclusively via eqn. (13) as expected [12] but the thermal reaction which produces the products shown in eqn. (13) and some $FeN_4(1\text{-MeIm})_2$ is too slow ($k = 4\times10^{-6}\,s^{-1}$) to allow one to unambiguously infer the reaction path in this case.

$$FeN_4X(CO)^- + 1\text{-MeIm} \longrightarrow FeN_4(1\text{-MeIm})_2 + X^- + CO \qquad (12)$$

$$FeN_4(CN)(CO)^- + 1\text{-MeIm} \longrightarrow FeN_4(1\text{-MeIm})(CN)^- + CO \qquad (13)$$

The *trans* effect order for CO loss from $FeN_4L(CO)$ is then: $MeIm < CN^- < py < 2\text{-MeIm}, CH_3CN < Br^-, Cl^-$.

TABLE 4. Comparison of kinetic data for the reaction of CO with some FeN_4L_2 systems

N	L	k_{-L}^{L} (s^{-1})	k_{-CO}^{L}	k_{+L}/k_{+CO}
$dmgBF_2$[a]	py	0.35	$2.7(0.6)\times10^{-5}$, d	15(2)
	MeIm	$2.8(0.2)\times10^{-3}$	$3(2)\times10^{-6}$, d	11(2)
	2-MeIm	160(20)	$2(0.1)\times10^{-4}$	22(5)
Pc[b]	py	0.12	0.09	3.4
	MeIm	2.6×10^{-3}	0.02	4.2
	2-MeIm	33	0.7	5.8
DHD[c]	Im	2×10^{5}	0.028	8.2
	2-MeIm		0.45	

[a]This work. MeIm and 2-MeIm data in CH_2Cl_2; py data in toluene at 25 °C. In pyridine k_{-CO}^{py} is reported as 3×10^{-5} s^{-1} and at 60 °C in toluene it is 6.4×10^{-3} s^{-1} [3a]. [b]Ref. 8 in toluene at 25 °C. [c]Ref. 7 in benzene at 23 °C. [d]Rate constants were determined from data over one half-life only.

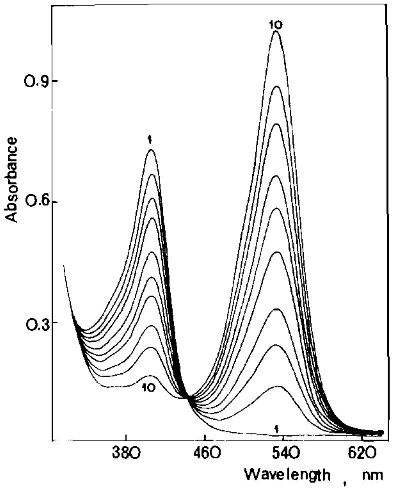

Fig. 4. Spectral changes with time for the reaction of $FeN_4(2\text{-MeIm})(CO)$ + MeIm in CH_2Cl_2 at 25 °C. Spectra 1–10 were recorded at times 0, 10, 20, 30, 48, 65, 80, 100, 140, 205 min, respectively.

The anion binding constants obtained here in CH_2Cl_2 containing 1.0 M CH_3CN are remarkably similar to those obtained in pure CH_3CN previously (comparison requires conversion to 1 M reference state for CH_3CN). Thus even for these anionic ligands, solvent effects are quite small as long as the equilibria concerned do not involve ions of opposite charge or have specific H-bonding or other effects. These results along with previous data [3] allow us to order the ligands in terms of their binding to $FeN_4(CH_3CN)_2$ as CO, CN^-, RNC > PBu_3 > $P(OEt)_3$ > MeIm > py > 2-MeIm ≫ Cl^- > Br^- > CH_3CN > dmso > dmf > thf. This list spans binding affinities over some 12 orders of magnitude.

Acknowledgement

We thank the Natural Sciences and Engineering Research Council of Canada for support.

References

1 I. W. Pang and D. V. Stynes, *Inorg. Chem.*, *16* (1977) 59.

2 (a) X. Chen and D. V. Stynes, *Inorg. Chem.*, *25* (1986) 1173.
(b) D. V. Stynes, D. Fletcher and X. Chen, *Inorg. Chem.*, *25* (1986) 3483.

3 (a) D. W. Thompson and D. V. Stynes, *Inorg. Chem.*, *29* (1990) 3815; (b) *30* (1991) 636; (c) D. G. A. H. de Silva, D. W. Thompson and D. V. Stynes, *Inorg. Chem.*, in press.

4 A. Butler and R. G. Linck, *Inorg. Chem.*, *23* (1984) 2227.

5 S. S. Eaton and G. R. Eaton, *Inorg. Chem.*, *16* (1977) 72.

6 F. Pomposo, D. Carruthers and D. V. Stynes, *Inorg. Chem.*, *21* (1982) 4245.

7 D. K. White, J. B. Cannon and T. G. Traylor, *J. Am. Chem. Soc.*, *101* (1979) 2443.

8 D. V. Stynes and B. R. James, *J. Am. Chem. Soc.*, *96* (1974) 2733.

9 J. P. Collman and C. A. Reed, *J. Am. Chem. Soc.*, *95* (1973) 2048.

10 (a) D. Brault and M. Rougee, *Biochemistry*, *14* (1975) 4100; (b) *Biochem. Biophys. Res. Commun.*, *57* (1974) 654; (c) G. C. Wagner and R. J. Kassner, *Biochim. Biophys. Acta*, *392* (1975) 319.

11 (a) W. R. Scheidt, J. F. Kirner, J. L. Hoard and C. A. Reed, *J. Am. Chem. Soc.*, *109* (1987) 1963; (b) W. R. Scheidt and C. A. Reed, *Chem. Rev.*, *81* (1981) 543.

12 X. C. Chen and D. V. Stynes, *Inorg. Chem.*, *26* (1987) 3145.